

Universal dielectric response of variously doped CeO₂ ionically conducting ceramics

A. S. Nowick, A. V. Vaysleyb, and I. Kuskovsky

Materials Science Division, School of Mines, Columbia University, New York, New York 10027

(Received 17 April 1998)

The Jonscher power law, or “universal dielectric response” (UDR) behavior was studied for a range of CeO₂ solid solutions with Y³⁺ and Gd³⁺ dopants, with particular emphasis on dilute systems which possess relatively simple defect structures. The results show power-law frequency dependence of the ac conductivity, with exponent $s = 0.61 \pm 0.03$, independent of temperature and concentration. The conductivity data also show scaling behavior in terms of a time constant τ , whose activation energy is very close to that of the dc conductivity. For 1% Y and 1% Gd samples, an additional Debye-type relaxation is observed due to dopant–oxygen-vacancy pairs. Such samples are clearly in the association range (stage III). These results contradict the assumption by Almond and West that τ^{-1} is the hopping frequency of the carrier defects. At very low concentrations ($\sim 0.01\%$), UDR behavior virtually disappears. The present results are then compared to the principal theories that describe UDR behavior. It is found that, while each theory suffers from some drawbacks, the more phenomenological theories fare better. [S0163-1829(98)09737-9]

I. INTRODUCTION

The measurement of the ac conductivity, σ , generally shows frequency dispersion, i.e., a dependence $\sigma(\omega)$ on the angular frequency ω . The study of this dispersive behavior offers an opportunity to gain insight into the details of ionic migration processes, particularly the interaction of the migrating ion with other defects in the structure.

It is well established that, in highly disordered systems, e.g., glasses, polymers, amorphous semiconductors and heavily doped crystals, over a wide range of frequencies, $\sigma(\omega)$ takes the form of a power law:

$$\sigma(\omega) = \sigma(0) + A\omega^s, \quad (1)$$

where $\sigma(0)$ is termed the “dc conductivity,” while the exponent s falls in the range $0.5 < s < 0.7$. Such behavior was first reported by Jonscher^{1,2} for such a wide variety of materials that he was led to denote this behavior as the “universal dielectric response,” UDR. Corresponding to Eq. (1), the imaginary part of the complex dielectric constant, ϵ^* , corresponding to UDR behavior is given by

$$\epsilon'' = [\sigma(\omega) - \sigma(0)] / \epsilon_0 \omega = (A / \epsilon_0) \omega^{-(1-s)}, \quad (2)$$

where ϵ_0 is the vacuum permittivity. Correspondingly, as a consequence of the Kramers-Kronig relation,² the real part of ϵ^* is given by

$$\epsilon' = \epsilon_\infty + (A / \epsilon_0) \tan(s\pi/2) \omega^{-(1-s)}, \quad (3)$$

where ϵ_∞ is the high-frequency value of $\epsilon'(\omega)$.

Clearly these power-law relations cannot be valid over the entire frequency range, since they give rise to divergences as $\omega \rightarrow 0$. It must therefore be recognized that UDR behavior is a high-frequency asymptotic form of a more general relation, such as the Cole-Davidson formula² for the complex permittivity:

$$\epsilon^* \approx (1 + i\omega\tau)^{-(1-s)}, \quad (4)$$

which gives rise to a peak in $\epsilon''(\omega)$, and a leveling off of $\epsilon'(\omega)$ at low frequencies.

A wide variety of theoretical approaches have been used to try to understand UDR behavior, in general, involving hopping of carrier ions with appropriate relaxation of surrounding ions in the crystal or glass structure.^{3–12} More will be said about these theories in the Discussion section.

Studies of $\sigma(\omega)$ at relatively high frequencies or low temperatures show a different power-law behavior in which an exponent close to unity appears and the conductivity is only weakly dependent on temperature. Since $s = 1$ means that ϵ'' is a constant, and since ϵ'' measures the energy loss per cycle, we refer to this regime as that of “nearly constant loss” (NCL). This NCL behavior has been found by many investigators for a diverse range of materials^{13–18} and, accordingly, has been termed a “second universality.”¹⁹ The two types of behavior, UDR and NCL, have been shown to superimpose, and are therefore regarded as due to separate mechanisms.²⁰ The NCL is generally regarded as resulting from relaxations involving a distribution of two-level systems, i.e., of particles moving in asymmetric double-well potentials.²¹ Such relaxation involves highly localized motions, rather than hopping processes. We will not deal with NCL behavior in this paper. Rather, it suffices to point out that, for the materials studied here, and for the available frequency window of these experiments (10–10⁵ Hz), UDR behavior is primarily observed above room temperature, and NCL sets in at lower temperatures.

The present work aims to study the effect of concentration of ionic carriers on UDR behavior, down to dilute systems. One question is whether the exponent s varies systematically with concentration. A second question, since UDR is related to defect interactions, is at how low a concentration UDR behavior ceases. Finally, the Almond-West assumption concerning the hopping frequency of the ionic carriers (to be discussed in the next section) will be tested. To accomplish these objectives, we have chosen a system of crystalline materials that is well studied and whose defect structure is relatively well understood, namely doped ceria, CeO₂:M³⁺, with

the 3+ dopants Y^{3+} and Gd^{3+} . These dopants substitute for Ce^{4+} to give defects $2M'_{Ce} + V_{\dot{O}}$ (in Kroger-Vink notation), i.e., two negatively charged dopant atoms compensated by a doubly positively charged oxygen-ion vacancy. The doped material is therefore an oxygen-ion conductor. For this system, much has previously been learned about the defect structure and about defect association (especially in the dilute range) through studies of the dc conductivity and of dielectric relaxation.²²⁻²⁴

II. RELATIONS AMONG QUANTITIES INVOLVED IN UDR

The theory of the dc conductivity, $\sigma(0)$, is well established.²⁴ It yields the following expression:

$$\sigma(0) = c_c N q^2 d^2 \nu_m / 6kT, \quad (5)$$

where c_c is the mole fraction of carriers, N the number of molecules/volume, q the charge on the carriers, d the hopping distance, and ν_m is the hopping frequency given by the Arrhenius expression:

$$\nu_m = \nu_0 \exp(-E_m/kT), \quad (6)$$

with E_m as the activation energy for migration or hopping. In general, due to association of carriers, c_c may be a function of temperature. There are two limiting cases to consider. If the carriers are unassociated, $c_c = c_0 = \text{const}$, where c_0 is the maximum carrier concentration based on the doping level. This case is variously known as the dissociation range, stage II behavior, or the strong electrolyte case. (The reader should recall that, in the terminology of stages of conductivity behavior, stage I represents the intrinsic region which, for doped oxides, would only exist at extremely high temperatures, i.e., close to the melting point.) The other extreme is where the carriers are strongly associated, and the concentration of free carriers c_c are those liberated by the dissociation reaction. In this case, known as the dissociation range, as stage III, or as the weak electrolyte, c_c is given by $c_c \sim \exp(-rE_a/kT)$, where E_a is the association energy and the numerical factor r is usually 1/2 or 1, depending on the defect system. (For $CeO_2:M^{3+}$, where association is primarily between a singly charged dopant M'_{Ce} and an oxygen-ion vacancy $V_{\dot{O}}$, $r=1$.²⁴) In either case, $\sigma(0)$ obeys the Arrhenius relation

$$\sigma(0)T = \alpha \exp(-E'_\sigma/kT), \quad (7)$$

with $E'_\sigma = E_m$ in the dissociation case, and $E'_\sigma = E_m + rE_a$ in the range of association.

It should be noted that we are adopting a notation in which a prime for an activation energy indicates that the quantity, x , under investigation is being plotted in the Arrhenius fashion as $\ln xT$ vs $1/kT$ to obtain E'_x . On the other hand, the unprimed "activation energy" E_x is obtained from a plot of $\ln x$ vs $1/kT$ which, over a limited range of T , would still give a good straight line. It is easy to see that these two energies are related by

$$E'_x = E_x + k\bar{T}, \quad (8)$$

where \bar{T} is the mean temperature in the region of measurement.

The quantity A of Eq. (1), representing the ac part of the conductivity, is also thermally activated, and we take it in the form:

$$A = (a/T) \exp(-E'_A/kT), \quad (9)$$

in which E'_A is the appropriate activation energy. Because of the awkward units of the quantity A , it has been advantageous to modify Eq. (1) into the equivalent form:

$$\sigma(\omega) = \sigma(0)[1 + (\omega\tau)^s], \quad (10)$$

thus defining a quantity τ , which we call the *ac relaxation time*, in place of A . Thus A and τ are related by

$$A = \sigma(0)\tau^s. \quad (11)$$

The temperature dependence of τ may then be given by

$$\tau = \tau_0 \exp(E_\tau/kT) \quad (12)$$

and, from Eq. (11), we obtain for the relations among the relevant activation energies and preexponentials:

$$E'_A = E'_\sigma - sE_\tau \quad (13)$$

and

$$\tau_0 = (a/\alpha)^{1/s}. \quad (14)$$

Almond and West^{25,26} not only wrote the UDR formula in the form of Eq. (10), but also made the assumption that the quantity τ^{-1} is equal to the hopping frequency, ν_m , of the dc conductivity. If true, this is a very important relationship, since it gives more than a phenomenological meaning to τ . Accordingly, one of the objectives of this paper will be to test this Almond-West assumption.

III. EXPERIMENTAL METHODS

Samples, in the form of disks 1 cm² in area and 1 mm thick, were prepared by solid state mixing, followed by calcining and sintering to a density >85% of theoretical. After cleaning and polishing the surfaces, guarded metallic electrodes of silver paste or sputtered gold were applied.

The conductance, G , and capacitance, C , were measured by an automated ac bridge (Andeen Associates, model CGA-83) adapted from a General Radio bridge, over the frequency range 10 Hz–100 kHz in 17 intervals. Data for $G(\omega)$ and $C(\omega)$ were converted, with the appropriate geometric factor, to conductivity $\sigma(\omega)$ in $(\Omega \text{ cm})^{-1}$, and relative dielectric permittivity $\epsilon'(\omega)$, respectively.

IV. RESULTS

We begin by examining Y-doped ceria, of the formula: $(1-x)CeO_2 \cdot xYO_{1.5}$. The material with $x=0.113$ (which we here refer to as 11.3% Y, but is often referred to as 6% Y_2O_3) is characteristic of the highly disordered systems studied earlier. Data for $\sigma(\omega)$ vs ω for this composition are plotted logarithmically in Fig. 1, showing a dc plateau leading into a power-law type behavior at each temperature. However, at the higher temperatures, the conductivity falls below

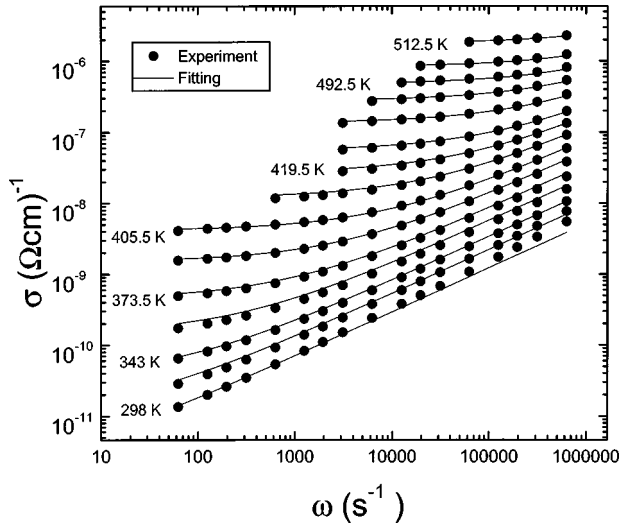


FIG. 1. Double logarithmic plot of the variation of σ with angular frequency ω for ceria containing 11.3% Y. Points are the measurements at various temperatures; curves are the fits with parameters given in Table I.

the dc value at low frequencies due to grain-boundary and electrode blocking effects.²⁷ There are two ways to handle this boundary effect. One is to insert additional parameters in the fitting equation to represent the effect; the other is simply to omit such data points from the fitting process. Since such boundary effects are complex and not of interest here, we have chosen the second of these alternatives and omitted the downturning points from Fig. 1.

As a first order estimate of $\sigma(0)$, the values of $\sigma(\omega)$ extrapolated to $\omega=1 \text{ sec}^{-1}$ are taken at each temperature (except for the three lowest temperatures) and then plotted as $T\sigma(0)$ vs $1/kT$ to obtain initial values of the Arrhenius parameters α and E'_σ [see Eq. (7)] to be used in computer fitting. Such Arrhenius plots are shown in Fig. 2 for the 11.3% Y composition as well as for two others.

The data of Fig. 1 are then fitted with 5 parameters: α , E'_σ , a , E'_A , and s , based on Eqs. (1), (7), and (9). (Note that we are taking the exponents s to be a constant, independent of frequency or temperature. This choice is based on preliminary plots of the data, temperature by temperature, which show no systematic variations of s , as well as past experience with this and other materials.^{20,28}) By utilizing only data above room temperature (298 K), it turned out unnecessary to introduce any terms to represent NCL behavior, although the lowest temperature (298 K) curve of Fig. 1 begins to show signs of NCL at high frequencies.

All parameters were iterated about initial values using nonlinear least-square fitting with statistical weighting to obtain the best fit to the data. (Statistical weighting is necessary, since the data span several orders of magnitude, both in σ and in ω .) We have used a standard procedure provided with the Microcal ORIGIN software package. Finally, the parameters so obtained were refined to obtain the best master curves, as described below.

The resulting parameters for this 11.3% Y composition are given in Table I. Also included are values of the parameters τ_0 and E_τ calculated from Eqs. (13) and (14). Note that E_τ is slightly larger than E'_σ , a result that had also been

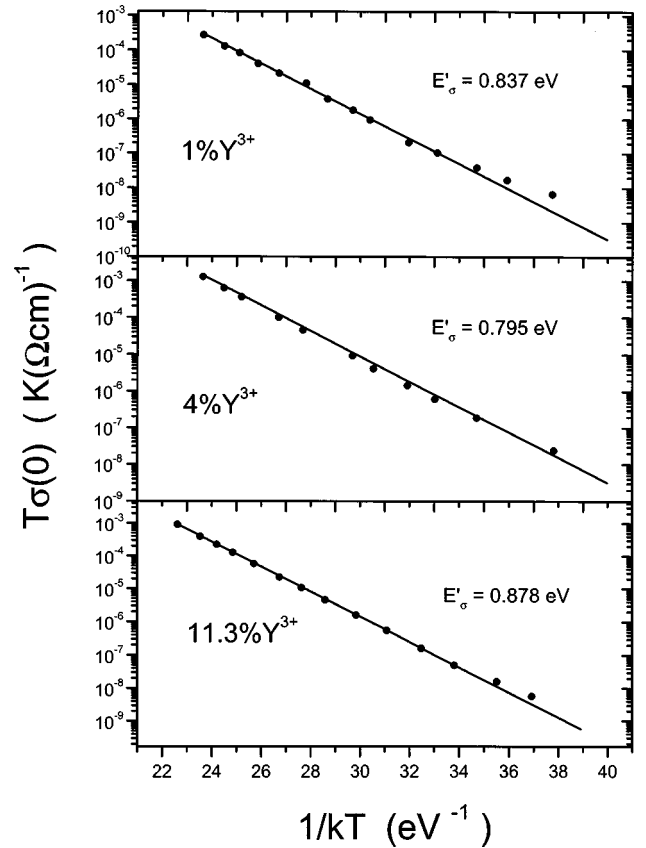


FIG. 2. Arrhenius plots of the dc conductivity, as $T\sigma(0)$ vs $1/kT$ for three Y dopings.

obtained previously,^{20,29} although it is difficult to say whether the small difference is experimentally significant. If E_τ were equal to E'_σ , it follows from Eq. (13) that $E'_A = (1-s)E'_\sigma$, a result that has often been reported for other materials in the past.^{30,31}

The concept of scaling comes from Eq. (10), which suggests that a plot of $\sigma(\omega)/\sigma(0)$ vs $\omega\tau$ will create a master curve from all of the data of Fig. 1. We tested this prediction by plotting logarithmically $[\sigma(\omega) - \sigma(0)]/\sigma(0)$ vs $\omega\tau$, as shown for the 11.3% sample in the top curve of Fig. 3. The quantity τ at each temperature was calculated from the Arrhenius parameters τ_0 and E_τ . Note that for $\sigma(\omega) < 2\sigma(0)$ (i.e., for $\omega\tau < 1$), there is an increase in slope, but a large scatter in the data. This is the range where the asymptotic power law changes into a more general form, such as the Cole-Davidson function of Eq. (4), but unfortunately the scatter in this region, where $\sigma(\omega)$ is so close to $\sigma(0)$, becomes so large that the detailed behavior is difficult to determine. For frequencies above this value, however, the power law applies over more than three decades of conductivity. The existence of such a master curve further supports the claim that the exponent s is very nearly independent of temperature.

It is highly desirable, simultaneously with $\sigma(\omega)$, to examine the data for $\epsilon'(\omega)$ for the same composition. Unfortunately, such data tend to be dominated by the effects of blocking at boundaries, resulting in a sharp upturn of $\epsilon'(\omega)$ toward lower frequencies, and only a very limited range of purely UDR behavior. Accordingly, we have fitted this data by using Eq. (3) with the parameters obtained from the $\sigma(\omega)$

TABLE I. Fitting parameters obtained from the ac conductivity data of the variously doped ceria samples.

Dopant	E'_σ (eV)	α $(\Omega \text{ cm})^{-1} \text{ K}$	E'_A (eV)	a $(\Omega \text{ cm})^{-1} (\text{sec})^s$	s	E_τ (eV)	τ_0^{-1} $(\text{sec})^{-1}$	B $\text{K}(\Omega \text{ cm})^{-1} \text{ sec}$	E_τ (eV)	τ_0^{-1} $(\text{sec})^{-1}$
1% Y	0.84	5.2×10^4	0.33	80×10^6	0.60	0.85	4.8×10^{14}	400	0.62	1.0×10^{13}
2% Y	0.81	8.5×10^4	0.32	120×10^6	0.59	0.83	1.0×10^{15}	800	0.61	1.2×10^{13}
4% Y	0.79 ₅	9.1×10^4	0.29	34×10^6	0.62	0.81 ₅	1.6×10^{15}	800	0.61	1.2×10^{13}
7.7% Y	0.87 ₅	60×10^4	0.31	58×10^6	0.62 ₅	0.90 ₅	1.1×10^{16}	200	0.61	1.0×10^{13}
11.3% Y	0.88	50×10^4	0.32 ₅	85×10^6	0.62 ₅	0.89	3.0×10^{15}			
1% Gd	0.73	2.4×10^4	0.28	39×10^6	0.60	0.75	4.4×10^{14}	20	0.45	1.0×10^{13}
2% Gd	0.70	3.3×10^4	0.27	78×10^6	0.59	0.73	4.1×10^{14}	40	0.50	1.2×10^{13}
11.3% Gd	0.81 ₅	31×10^4	0.32	197×10^6	0.60	0.83	2.1×10^{15}	25	0.45	1.1×10^{13}
“undoped”	0.81 ₅	1.3×10^4	0.41	72×10^6	0.59	0.69	1.0×10^{14}	55	0.57 ₅	0.5×10^{13}

fitting, leaving only ε_∞ open. This parameter was allowed to vary linearly with temperature, as:

$$\varepsilon_\infty = \varepsilon_1 + \gamma T. \quad (15)$$

Figure 4 shows the data and the results of this fitting, including an inset showing the high-frequency regions enlarged. The results give $\varepsilon_1 = 20.2$ and $\gamma = -0.0008 \text{ K}$, indicating that the temperature dependence of ε_∞ may not actually be significant.

In the study of $\varepsilon'(\omega)$ for a silicate glass,²⁰ a decrease in slope toward low frequencies clearly appeared, corresponding to the onset of a more general behavior such as the Cole-Davidson, Eq. (4). In the present case, such a turndown is not evident. Perhaps the failure to observe this effect here is due to grain-boundary blocking, which sets in before the electrode blocking effects (as a second arc in the complex impedance plot).²⁷ Such an effect is, of course, absent for glasses.

We turn now to our most dilute Y-doped sample, that containing 1% Y. The data for $\sigma(\omega)$ vs ω are shown in Fig.

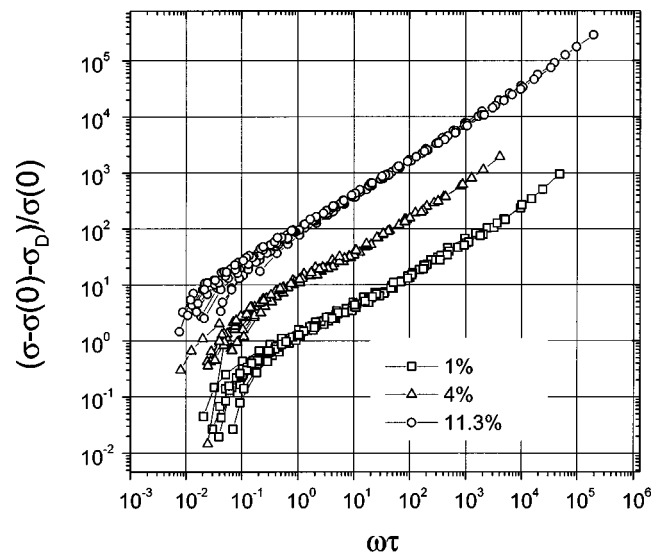


FIG. 3. Use of scaling to create master plots. Here $[\sigma(\omega) - \sigma(0)]/\sigma(0)$ is plotted vs $\omega\tau$ for three ceria compositions. (A Debye relaxation term, σ_D , is only used for the 1% and 4% compositions, and for these, it is subtracted out.) To separate the curves, the ordinates of the two top curves are multiplied by a scale factor: $\times 10$ for the 4% curve and $\times 100$ for the 11.3% curve.

5, and the Arrhenius plot in Fig. 2. Clearly, the behavior is more complex than that of the 11.3% sample, in the appearance of steps in the $\sigma(\omega)$ curves below $\sim 400 \text{ K}$. In view of Eq. (2), a step in this curve corresponds to a peak in the dielectric loss, $\varepsilon''(\omega)$. The peaks may be seen in Fig. 6, which plots $\varepsilon''(\omega)$ for the four lowest temperatures, where they fall in the region $\omega = 1000$ to $30\,000 \text{ s}^{-1}$. A simple Debye peak in ε'' translates into a contribution to $\sigma(\omega)$ of the form:

$$\sigma_D = (B/T)(\omega^2 \tau_r)/(1 + \omega^2 \tau_r^2), \quad (16)$$

with relaxation time τ_r , and relaxation strength $\Delta\varepsilon$, and where $B = \varepsilon_0 \Delta\varepsilon T$. The existence of a dielectric loss peak for this composition is well known, and has been studied in considerable detail.²² (A matching anelastic relaxation peak has also been studied.³²) The peak was shown to be due to bound pairs consisting of a Y' dopant and an oxygen-ion vacancy, $V_{\text{O}}^{\cdot\cdot}$, where the pair $YV_{\text{O}}^{\cdot\cdot}$ possesses a net positive charge. Figure 6 also shows the presence of a broad additional peak on the low-frequency side of the Debye peak. This peak has also been studied²² and shown to be due to relaxation of the array of charged defects: Y' and $YV_{\text{O}}^{\cdot\cdot}$. In fitting the data of Fig. 5, we used the same five parameters as for the 11.3% sample, but in addition we added a term σ_D , of the type given by Eq. (16), with three new parameters: B , τ_{r0} , and E_r , where we take τ_r in the Arrhenius form:

$$\tau_r = \tau_{r0} \exp(E_r/kT). \quad (17)$$

This procedure takes into account the principal relaxation peak, but ignores the broader low-frequency relaxation. Initial values for the activation energy E_r were obtained from the Arrhenius plot of the peak position as a function of temperature, while initial values of the parameter B were obtained from the peak magnitude. The results of the fitting are shown by the solid curves of Fig. 5, and the parameters obtained are listed in Table I. Note that the value of E_r obtained is 0.61 eV, considerably smaller than the value 0.84 eV for E'_σ . This result for E_r is in good agreement with the work of Wang,²² who studied the dielectric loss phenomenon using a quasistatic method, as well as that of Funke *et al.*³³ The value of τ_{r0} is also close to 10^{-13} sec , as expected.

The master curve for this 1% composition, is given in Fig. 3 with the Debye relaxation term, σ_D , subtracted out. It shows a somewhat narrower UDR range than the 11.3%

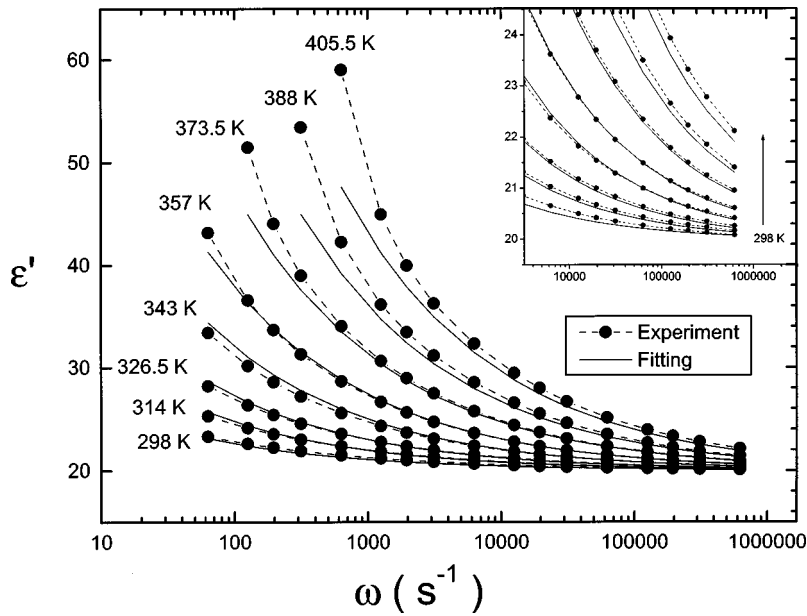


FIG. 4. Variation of $\epsilon'(\omega)$ with ω for ceria containing 11.3% Y. The inset is an enlargement of the high-frequency region. Dashed curves simply connect the experimental points, while solid curves are the fits with the parameters of Table I.

sample, extending only to the mid 10^4 range in $\omega\tau$, and showing greater scatter, but the slope s is virtually unchanged at 0.60. The turn-up at the highest $\omega\tau$ values may represent the beginning of NCL behavior.

The remaining compositions of 2%, 4% and 7.7% Y are then filled in, including a dielectric relaxation term of the type of Eq. (16). (The use of a pure Debye term is somewhat imperfect, since we know from previous work that the relaxation peak broadens considerably for compositions above 1% Y.) The results of the fitting are given in Table I, and the master curve for the 4% material is included in Fig. 3. Note that the magnitude, B , of the relaxation peak doubles in going from 1% to 2% Y, but falls off at higher concentrations, showing the effect of peak broadening.

It is important to note that the three master curves shown in Fig. 3 are identical to within experimental error. We have plotted them with displaced scales to avoid overlap of data.

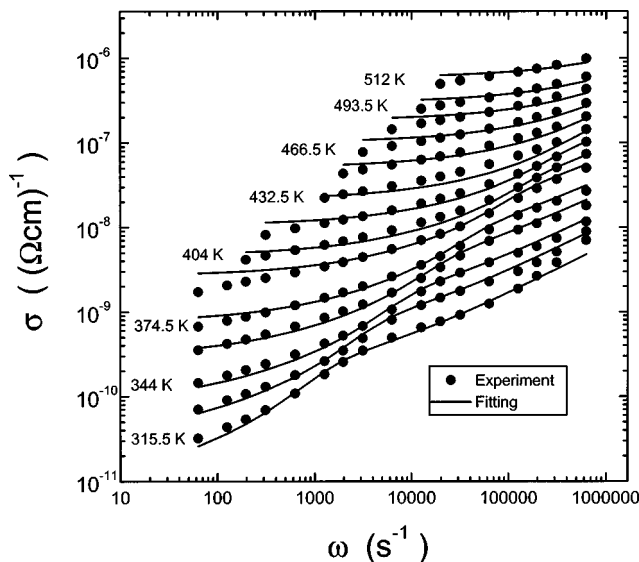


FIG. 5. Log-log plot of $\sigma(\omega)$ vs ω for ceria-1% Y, comparing experimental points to a fitted curve that now includes a Debye-relaxation term.

However, if all the data were plotted on one scale, it would give rise to a ‘super’ master curve. A similar result was obtained by Kahnt.³⁴ It differs from the super-master curve of Roling *et al.*,³⁵ who plotted $\sigma(\omega)/\sigma(0)$ vs $\omega x/T\sigma(0)$, where x is the dopant fraction for a series of Na-borate glasses, to obtain such a supermaster curve. The present case does not incorporate the concentration into the abscissa, and, in fact, would not give a single curve if that were done.

In a similar way, samples doped with 1%, 2%, and 11.3% Gd are studied. For these samples, we find a relaxation peak at lower temperatures than for the Y-doped samples. Also present is a second peak at an activation energy of ~ 0.60 eV, but this is poorly defined, and therefore ignored in the fitting. Results for these samples are summarized in Table I. Note that E'_σ is distinctly lower for 1% and 2% Gd than it is for the corresponding Y concentrations, in agreement with previous work by Gerhardt.³⁶

In view of the existence of UDR behavior at compositions of 1% Y or Gd, we sought a more dilute system. Since a

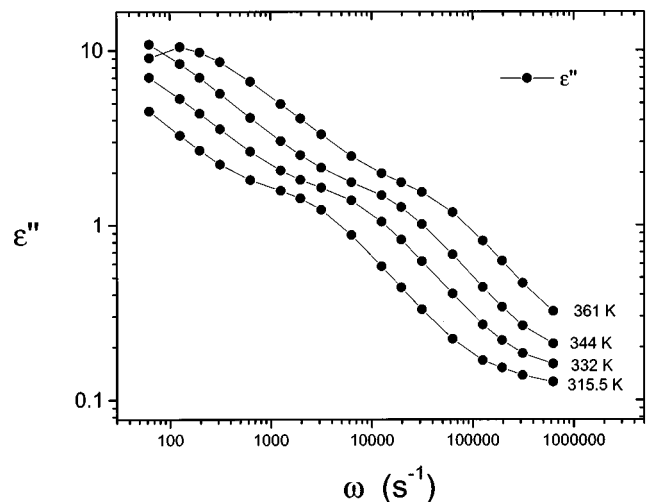


FIG. 6. Plot of $\epsilon''(\omega)$ vs ω for the four lowest temperatures of Fig. 5, showing the presence of relaxation peaks. The drawn curves here are only guides to the eye.

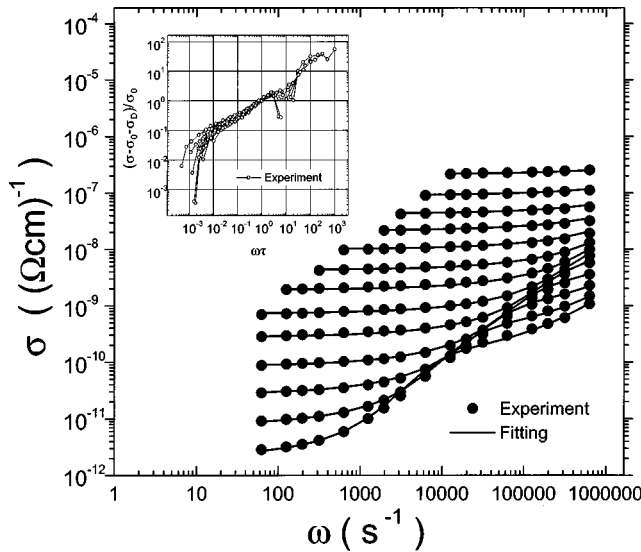


FIG. 7. Log-log plot of $\sigma(\omega)$ for nominally “undoped” ceria. Fitting includes a Debye relaxation. The inset represents an attempt to produce a master curve.

homogeneous sample of much lower Y or Gd content was unavailable, we turned instead to an “undoped” sample which was not of high purity (presumably with \sim several hundredths % of aliovalent impurity). The data for $\sigma(\omega)$ for this sample are shown in Fig. 7, and the fitted parameters are given in Table I. The conductivity level is about an order of magnitude lower than for the doped samples, but there is still a relaxation peak at the lower temperatures. The master plot, given as an inset to the figure, shows a power-law region with $s=0.6$ over, at most, one order of magnitude. It may therefore be concluded that a well-defined UDR region no longer exists for this composition.

V. DISCUSSION

The principal results of the present study may be summarized as follows.

(1) The UDR exponent, s , is apparently independent of frequency, temperature, and composition in the ranges studied, having a value $s=0.61 \pm 0.03$. This value is strikingly close to the exponent obtained for other ionically conducting materials, including glasses.^{20,28,34,37–39}

(2) The time constant, τ , that represents the ac behavior [Eq. (10)], consistently has an activation energy, E_τ , slightly higher than that of the dc conductivity, E'_σ , by ~ 0.02 eV. This result agrees with a similar finding for other ionically conducting materials.^{20,29} Note that if E_τ were instead compared to E_σ (unprimed), it would be definitely higher, in view of the extra term $kT \sim 0.035$ eV. [See Eq. (8).] The preexponential, τ_0^{-1} , is close to 10^{15} sec $^{-1}$, which is much higher than phonon frequencies.

(3) At low dopant concentrations, particularly 1% Y or Gd, the ac conductivity is complicated by the appearance of dielectric loss peaks. This result confirms earlier studies, both of dc conductivity²³ and of dielectric relaxation,²² showing that the conductivity is in the association range (weak electrolyte). In addition, the substantial difference in E'_σ between the 1% Gd and the 1% Y samples (0.73 and 0.84

eV, respectively), further supports this conclusion, since such a large difference can only be reasonably interpreted as a difference in association energy, E_a , for these two dopants of different ionic radius.²⁴ Nevertheless, when the relaxation contribution to the conductivity is subtracted out, the UDR behavior of these low-concentration samples is similar to that for high concentrations, although the range is smaller.

(4) At very low defect concentrations, characterized by the present “undoped” sample, UDR behavior virtually disappears, although $\sigma(0)$ continues to show Arrhenius behavior. Such a result has also been found for very dilute glasses, for which the claim has been made that $s \rightarrow 0$.^{40–44}

In examining these results, special attention must be paid to the results for 1% Y and 1% Gd-doped samples. Here we have considerable evidence for strong association, with a well-defined defect structure consisting MV_O pairs and an equal number of unassociated M' defects. Detailed analysis of the dc conductivity as a function of temperature²³ shows that the migration energy E_m is close to 0.61 eV, while the remainder of E'_σ is the association energy E_a . Thus, the observation that $E_\tau \cong E'_\sigma$ means that τ^{-1} cannot be the hopping frequency of the carrier defects, as Almond and West had assumed. The high value of τ_0^{-1} ($\sim 10^{15}$ sec $^{-1}$) and its strong dependence on concentration (see Table I), also constitute strong arguments against the Almond-West assumption.

From our knowledge of the defect structure for these dilute compositions, we may expect that the existence of UDR behavior may stem from the migration of V_O carriers through a “Coulombic mine field” of M' and MV_O charges. On this basis, results for CeO₂ doped with divalent cations (e.g., Ca²⁺), where the CaV_O defect pairs are neutral, might turn out to be quite different.

There are many theories that attempt to explain UDR behavior.^{3–12} These theories start with widely different assumptions about the nature of defect interactions. Some theories are macroscopic in nature; others look at the detailed atomic jump processes. Since all of them predict a power-law frequency dependence of the ac conductivity, it is difficult to test them based on the usual ac conductivity measurements. The present work offers such an opportunity because we know a great deal about the defect structure of the doped ceria compounds, particularly those of low concentrations. Accordingly, in the remainder of this Discussion, we shall briefly review some widely cited theories of dispersive ac behavior to compare their predictions with the present results, as summarized above. In view of the materials studied here, we limit ourselves to theories suitable to crystalline materials, since many previous authors were focused on glasses. We begin with the more macroscopic or phenomenological theories, and then move toward those that are more specific or atomistic.

The *random free-energy barrier model*, as described by Dyre⁶ is based on earlier work by Scher and Lax.⁴⁵ In this approach, the defect interactions of a disordered material are simulated by spatially randomly varying free-energy barriers for the hopping charge carriers. Such a hopping model can be solved in two different approximations: the continuous time random walk, and the effective medium approximations, both of which give almost identical solutions at high

frequencies (i.e., in the UDR domain). The ac and dc behaviors are due to the same mechanism, with $\sigma(0)$ determined by the existence of continuous percolation paths through the material, while the ac part involves more limited motions. The model predicts a universal shape of $\sigma(\omega)$ in scaling coordinates: $\ln \sigma/\sigma(0)$ vs $\ln \omega\tau$, and that τ^{-1} and $\sigma(0)$ are related through the so-called BNN relation:⁴⁶

$$\sigma(0) = p\varepsilon_0\Delta e/\tau. \quad (18)$$

Here Δe is a dimensionless relaxation strength, which varies as $1/T$, while p is a constant of order unity. It is therefore predicted that $E_\tau = E'_\sigma$, which is close to the results that we obtain. Further there appears to be no reason why the theory should be limited to strong electrolytes. However, the theory gives no information on the existence of a cutoff to UDR behavior at low concentrations. Finally, in this theory, the exponent s is predicted to be temperature dependent, rather than constant, and in fact, $s \rightarrow 1$ as $T \rightarrow 0$ as a linear function of temperature, which we do not observe.

In a later paper, Dyre⁴⁷ has proposed a ‘‘macroscopic model,’’ in which he obtains an equivalent electrical circuit by discretizing Maxwell’s equations. The results are not very different from those of the hopping model.

The *coupling model* of Ngai^{4,5} expresses relaxation behavior due to defect interactions in the time domain by a correlation function $\phi(t)$, which is the relaxation of the electric field at constant displacement vector, D . For very short times this function is exponential, involving a time constant whose activation energy is a ‘‘primitive value’’ E_p , representing what is claimed to be the true one-particle energy barrier for hopping. On the other hand, as a result of relaxation, for longer times, $\phi(t)$ becomes a stretched exponential (the so-called KWW function): $\phi(t) = \exp(-t/\tau)^\beta$, where $\beta = (1-s)$. The quantity s is called the coupling parameter, and measures the strength of the interactions. (In the absence of coupling, $s=0$.) When converted into the frequency domain, the theory predicts, for large $\omega\tau$, a power-law variation of $\sigma(\omega)$, with the ac activation energy, E_A , equal to E_p . It also obtains, for the dc activation energy: $E'_\sigma = E_p/(1-s)$.

If we introduce the Maxwell relaxation time, τ_{dc} , as that given by $\sigma(0) = \varepsilon_0\varepsilon_s/\tau_{dc}$, where ε_s is the permittivity of the medium, this theory gives for the ac conductivity relaxation time τ , the relation:

$$\tau = \beta\tau_{dc}/\Gamma(1/\beta), \quad (19)$$

where Γ is the gamma function. The theory therefore predicts that $E_\tau = E_\sigma$ (unprimed). This represents a discrepancy with the present results which show that E_τ is even slightly larger than E'_σ , and therefore certainly larger than E_σ . Further, for the dilute ceria solid solutions studied here, the coupling model would require that the ac activation energy, E_A , which is ~ 0.3 eV, represents the primitive hopping energy, E_p . Considering that the activation energy, E_r , for the simple reorientation of a bound Y- V_O pair is 0.61 eV, and that for a Gd- V_O pair is 0.45 eV (see Table I), a value of 0.3 eV may be unrealistically small for a hopping energy in this

system. Finally, for sufficiently dilute systems, this theory predicts that $s \rightarrow 0$, i.e., disappearance of UDR behavior.

The *jump relaxation model* of Funke⁸ proposes that the conductivity dispersion can be understood in terms of Debye-Hückel type interactions between a hopping ion and surrounding defects. A given ion at site A can move to an adjacent vacancy at site B over an activation barrier. In general, the cage-effect potential due to Coulombic interactions, is less favorable at site B than it was at site A , so that the hopping ion is biased to return. However, there will be a relaxational response of the surrounding environment, which tries to accommodate the new location of the hopping ion. This all leads to a correlated forward-backward hopping process, i.e., to the occurrence of ‘‘unsuccessful jumps’’ that contribute only to the ac, and not the dc conductivity, and to a power-law dispersion in the appropriate frequency range. The power-law exponent $s = 1 - \beta$, where β indicates the mismatch between potential energies of the two wells. The dc activation energy, E'_σ , corresponds to hopping after the surrounding environment has relaxed, and it is related to the ac activation energy (here, E'_A) by: $E'_\sigma = \beta E'_\sigma = (1-s)E'_\sigma$. The time constant t_2 that controls the onset of the relaxation process (corresponding to our τ) is roughly equal to the rate of successful hops, and is thermally activated with the energy for successful hops E'_σ .

In this form, the jump relaxation theory yields the Almond-West assumption, and leaves no room for an association energy, E_a , as part of E'_σ , i.e., for dealing with a weak electrolyte.

The *lattice-gas model* of Bunde, Dieterich and others^{11,12} uses Monte Carlo methods to simulate diffusion of charged particles on a disordered lattice. The disorder is produced by site percolation, where the percolation cluster represents the allowed positions for ions, and the remaining sites are forbidden. The method gives rise to nonclassical diffusion, and correspondingly, to conductivity dispersion, only when disorder is augmented by Coulombic interactions. As in the jump-relaxation model, correlated forward-backward hops are found to be responsible for the ac conductivity, with a sub-linear frequency exponent s . The quantity s is found to increase substantially as T decreases and also to increase as the strength of the Coulombic interaction decreases (i.e., as the concentration of dopant goes down). Finally, the crossover frequency, $1/\tau$, between the dc and ac regions is found to be activated with the activation energy E'_σ , thus supporting the Almond-West assumption. It is clear that, while this theory provides very detailed information on the atomistics of the hopping process, its predictions in terms of the present experimental results are flawed.

By interpreting the present results in terms of these various theories, it may be concluded that, in general, the more phenomenological theories fare better than those taking a detailed atomistic approach.

There have been more recent modifications of the above theories,^{48,49} but these yield no major differences in predictions relative to the present experiments. However, an additional theory of the phenomenological type is worthy of mention. The *dynamic cluster model* suggested by one of us⁵⁰ (A.V.V.) is based on an analysis of Efros and Shklovskii.⁵¹ It makes the grossly oversimplified assumption

that there exist just two different regions of the crystal: region 1, consisting of more highly conducting clusters, are imbedded in a matrix known as region 2. The corresponding activation energies for conduction in the two regions are E_1 and E_2 , respectively. With a decrease in frequency, the volume of region 1 clusters increases until they overlap and percolation occurs. The conductivity relaxation time, τ , is related to the Maxwell relaxation time of region 2. Thus, $E_\tau = E_2$, while the dc conductivity is given by $E'_\sigma = \nu_c E_1 + (1 - \nu_c) E_2$, where ν_c is the fraction of material in region 1 at percolation. Thus E_τ may indeed be slightly larger than E'_σ . Finally, the model gives an explicit concentration threshold below which UDR behavior is not observed. Such behavior requires that, for UDR behavior, W/kT should be ≥ 1 , where W is the repulsive Coulomb energy of mobile carriers. Since W depends on the concentration, a threshold

concentration may be calculated. The result gives, for the concentration of carriers below which UDR behavior ceases, the value $n^* \sim r_{\text{On}}^{-3}$, where r_{On} is the ‘‘Onsager radius’’ $= q^2/\epsilon_s kT$. Here q is the charge on the defects. For CeO_2 , this gives a concentration (as a mole fraction) $\sim 3 \times 10^{-4}$, consistent with the disappearance of UDR in the case of the ‘‘undoped’’ sample. It also predicts that this critical concentration becomes much larger in a material of high dielectric permittivity.

ACKNOWLEDGMENTS

The authors are grateful to Dr. Himanshu Jain, Dr. Allen Hunt, and Dr. J. Ross Macdonald for valuable discussions and to the U.S. Department of Energy for support of this work.

- ¹A. K. Jonscher, *Nature (London)* **267**, 673 (1977).
- ²A. K. Jonscher, *Dielectric Relaxation in Solids* (Chelsea Dielectrics Press, London, 1983).
- ³M. Pollak and G. E. Pike, *Phys. Rev. Lett.* **28**, 1449 (1972).
- ⁴K. L. Ngai, *Comments Solid State Phys.* **9**, 127 (1979); **9**, 141 (1980).
- ⁵K. L. Ngai, R. W. Rendell, A. K. Rajagopal, and S. Teitler, *Ann. (N.Y.) Acad. Sci.* **484**, 150 (1986).
- ⁶J. C. Dyre, *J. Appl. Phys.* **64**, 2456 (1988).
- ⁷L. A. Dissado and R. M. Hill, *J. Appl. Phys.* **66**, 2511 (1989).
- ⁸K. Funke, *Z. Phys. Chem., Neue Folge* **154**, 251 (1987); *Prog. Solid State Chem.* **22**, 111 (1993).
- ⁹S. R. Elliott and A. P. Owens, *Philos. Mag. B* **60**, 777 (1989).
- ¹⁰A. Hunt, *J. Phys.: Condens. Matter* **3**, 7831 (1991); *J. Non-Cryst. Solids* **160**, 183 (1993).
- ¹¹P. Maass, J. Petersen, A. Bunde, and W. Dieterich, *Phys. Rev. Lett.* **66**, 52 (1991).
- ¹²P. Maass, M. Meyer, and A. Bunde, *Phys. Rev. B* **51**, 8164 (1995).
- ¹³J. Wong and C. A. Angell, *Glass Structure by Spectroscopy* (Dekker, New York, 1976), p. 750.
- ¹⁴A. R. Long, *Adv. Phys.* **31**, 553 (1982).
- ¹⁵S. R. Elliott, *Adv. Phys.* **36**, 135 (1987); *Solid State Ionics* **70-71**, 27 (1994).
- ¹⁶B. S. Lim, A. V. Vaysleyb, and A. S. Nowick, *Appl. Phys. A: Solids Surf.* **A56**, 8 (1993).
- ¹⁷X. Lu and H. Jain, *J. Phys. Chem. Solids* **55**, 1433 (1994).
- ¹⁸D. L. Sidebottom, P. F. Green, and R. K. Brow, *J. Non-Cryst. Solids* **203**, 300 (1996).
- ¹⁹W. K. Lee, J. F. Liu, and A. S. Nowick, *Phys. Rev. Lett.* **67**, 1559 (1991).
- ²⁰A. S. Nowick, A. V. Vaysleyb, and Wu Liu, *Solid State Ionics* **105**, 121 (1998).
- ²¹S. Estalji, O. Kanert, J. Steinert, H. Jain, and K. L. Ngai, *Phys. Rev. B* **43**, 7481 (1991).
- ²²D. Y. Wang and A. S. Nowick, *J. Phys. Chem. Solids* **44**, 639 (1983).
- ²³D. Y. Wang, D. S. Park, J. Griffith, and A. S. Nowick, *Solid State Ionics* **2**, 95 (1981).
- ²⁴A. S. Nowick, in *Diffusion in Crystalline Solids*, edited by G. M. Murch and A. S. Nowick (Academic Press, Orlando, 1985), Chap. 3.
- ²⁵D. P. Almond, G. K. Duncan, and A. R. West, *Solid State Ionics* **8**, 159 (1983).
- ²⁶D. P. Almond, C. C. Hunter, and A. R. West, *J. Mater. Sci.* **19**, 3236 (1984).
- ²⁷D. Y. Wang and A. S. Nowick, *J. Solid State Chem.* **35**, 325 (1980).
- ²⁸W. K. Lee, B. S. Lim, J. F. Liu, and A. S. Nowick, *Solid State Ionics* **53-56**, 831 (1992).
- ²⁹A. S. Nowick, B. S. Lim, and A. V. Vaysleyb, *J. Non-Cryst. Solids* **172-174**, 1243 (1994).
- ³⁰S. W. Martin and C. A. Angell, *J. Non-Cryst. Solids* **83**, 185 (1986).
- ³¹K. L. Ngai, *J. Non-Cryst. Solids* **203**, 232 (1996).
- ³²M. P. Anderson and A. S. Nowick, *J. Phys. (Paris), Colloq.* **42**, C5-823 (1981).
- ³³K. Funke, T. Maue, D. Wilmer, C. Cramer, and T. Saatkamp, in *Ionic and Mixed Conducting Ceramics*, Proceedings of the Second Conference, edited by T. Ramanarayanan (The Electrochem. Society, New York, 1994), p. 564.
- ³⁴H. Kahnt, *Ber. Bunsenges. Phys. Chem.* **95**, 1021 (1991).
- ³⁵B. Roling, A. Happe, K. Funke, and M. D. Ingram, *Phys. Rev. Lett.* **78**, 2160 (1997).
- ³⁶R. Gerhardt and A. S. Nowick, *J. Am. Ceram. Soc.* **69**, 641 (1986).
- ³⁷H. Jain and J. M. Mundy, *J. Non-Cryst. Solids* **91**, 955 (1991).
- ³⁸A. Pradel and M. Ribes, *J. Non-Cryst. Solids* **131-133**, 1063 (1991).
- ³⁹D. L. Sidebottom, P. F. Green, and R. K. Brow, *Phys. Rev. Lett.* **74**, 5068 (1995).
- ⁴⁰K. L. Ngai and S. W. Martin, *Phys. Rev. B* **40**, 10550 (1989).
- ⁴¹J. F. Cordaro and M. Tomozawa, *J. Am. Ceram. Soc.* **64**, 713 (1981).
- ⁴²O. Kanert, J. Steinert, H. Jain, and K. L. Ngai, *J. Non-Cryst. Solids* **131-133**, 1001 (1991).
- ⁴³H. Patel and S. W. Martin, *Phys. Rev. B* **45**, 10292 (1992).
- ⁴⁴H. Jain and S. Krishnawami, *Solid State Ionics* **105**, 129 (1998).
- ⁴⁵H. Scher and M. Lax, *Phys. Rev. B* **7**, 4491 (1973); **7**, 4502 (1973).
- ⁴⁶M. Tomozawa, in *Treatise on Materials Science and Technology*,

- edited by M. Tomozawa and R. H. Doremus (Academic Press, New York, 1977), Vol. 12, p. 283.
- ⁴⁷J. C. Dyre, Phys. Rev. B **48**, 12 511 (1993).
- ⁴⁸A. Bunde, K. Funke, and M. D. Ingram, Solid State Ionics **86-88**, 1331 (1996).
- ⁴⁹P. Pendzig and W. Dieterich, Solid State Ionics **105**, 209 (1998).
- ⁵⁰A. V. Vaysleyb, following paper, Phys. Rev. B **58**, 8407 (1998).
- ⁵¹A. L. Efros and B. I. Shklovskii, Phys. Status Solidi B **76**, 475 (1976).